

1
2 Supplementary Materials for
3

4 Modulation of the relationship between summer temperatures in the Qinghai–
5 Tibetan Plateau and Arctic over the past millennium by external forcings
6

7 Feng Shi^{1,2,*}, Anmin Duan^{3,4}, Qiuzhen Yin⁵, John T Bruun^{6,7}, Cunde Xiao⁸, Zhengtang Guo^{1,2,4}

8 ¹Key Laboratory of Cenozoic Geology and Environment, Institute of Geology and Geophysics,
9 Chinese Academy of Sciences, Beijing 100029, China.

10 ²CAS Center for Excellence in Life and Paleoenvironment, Beijing 100044, China.

11 ³State Key Laboratory of Numerical Modelling for Atmospheric Sciences and Geophysical Fluid
12 Dynamics (LASG), Institute of Atmospheric Physics (IAP), Chinese Academy of Sciences,
13 Beijing 100029, China.

14 ⁴University of Chinese Academy of Sciences, Beijing 100049, China.

15 ⁵Georges Lemaître Centre for Earth and Climate Research, Earth and Life Institute, Université
16 Catholique de Louvain, Louvain-la-Neuve 1348, Belgium.

17 ⁶College of Engineering, Mathematics and Physics Sciences, University of Exeter, Exeter, UK.

18 ⁷College of Life and Environmental Sciences, University of Exeter, Penryn Campus, Penryn,
19 UK.

20 ⁸State Key Laboratory of Earth Surface Processes and Resource Ecology, Beijing Normal
21 University, Beijing 100875, China

22 ⁹University of Chinese Academy of Sciences, Beijing 100049, China.

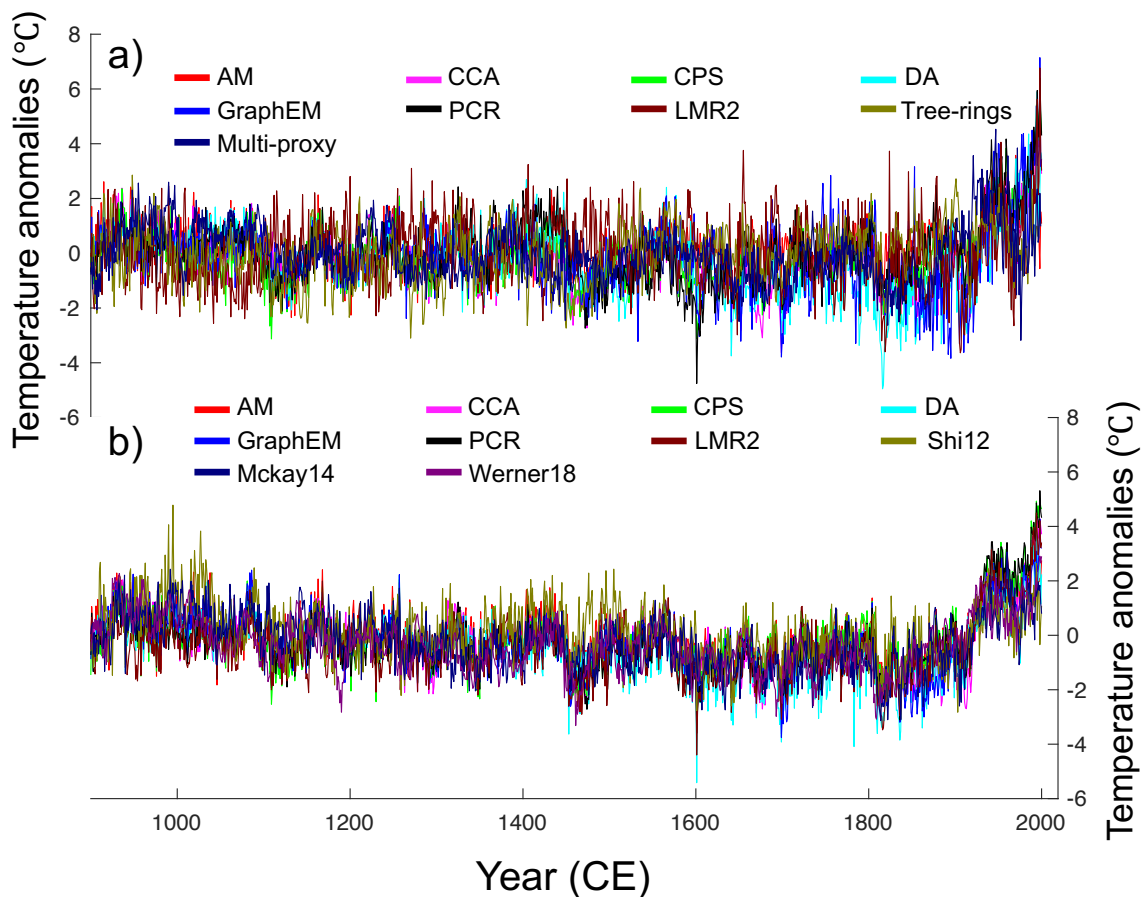
23 *Correspondence to: shifeng@mail.iggcas.ac.cn

24

25

26 This PDF file includes 6 figures to clarify our results.

27



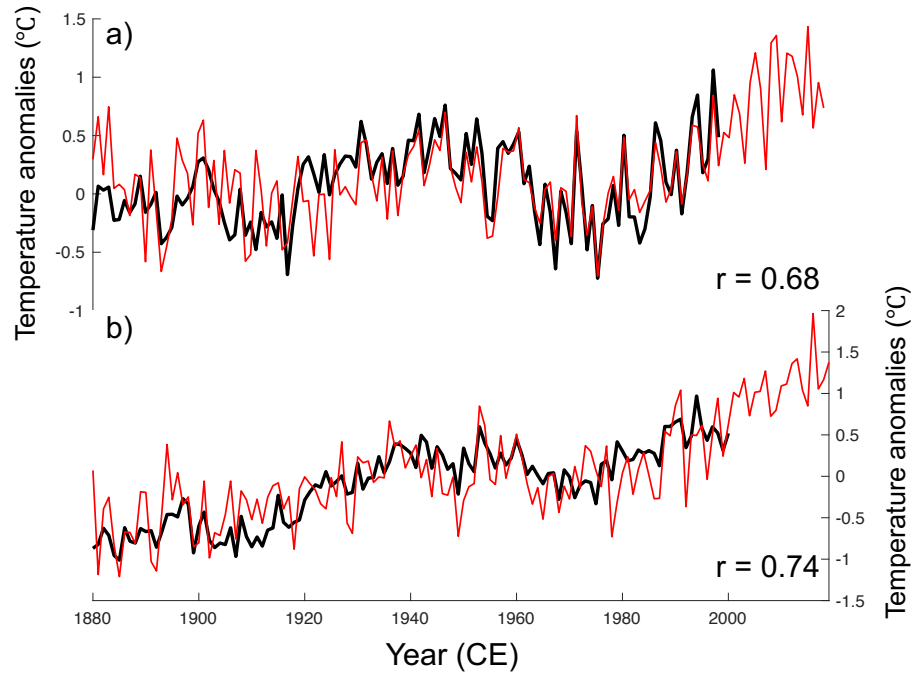
28

29 **Fig. S1.** Comparison of reconstructed temperature anomalies (unit: °C, with respect to 1961–
 30 1990 CE) over the past millennium (900–2000 CE) in the (a) Qinghai–Tibetan Plateau and (b)
 31 Arctic based on different reconstructions.

32

33

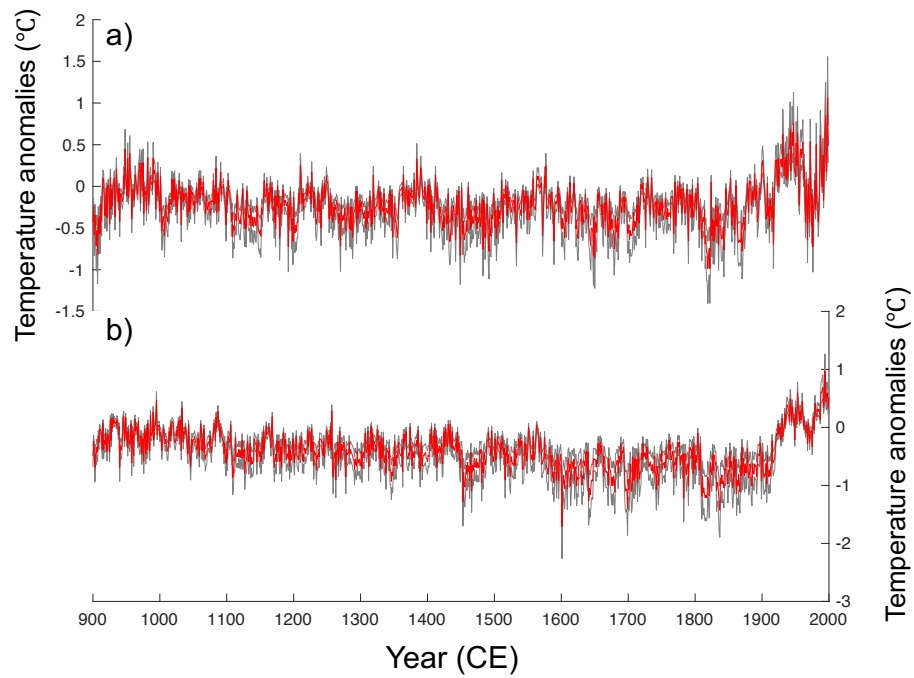
34



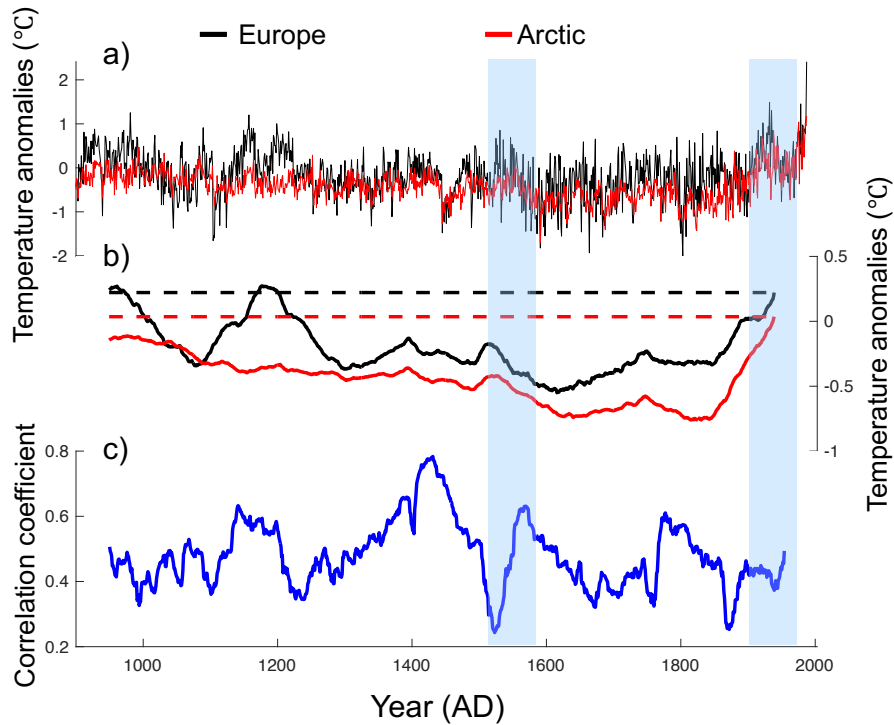
35

36 **Fig. S2.** Comparison of the reconstructed and instrumental summer temperature anomalies (unit:
37 °C, with respect to 1961–1990 CE) used in this study over the period 1880–1999 CE in the (a)
38 Qinghai–Tibetan Plateau and (b) Arctic. The red and black lines are the instrumental and proxy
39 reconstructed data, respectively, and their correlation (r) is shown in each panel.

40



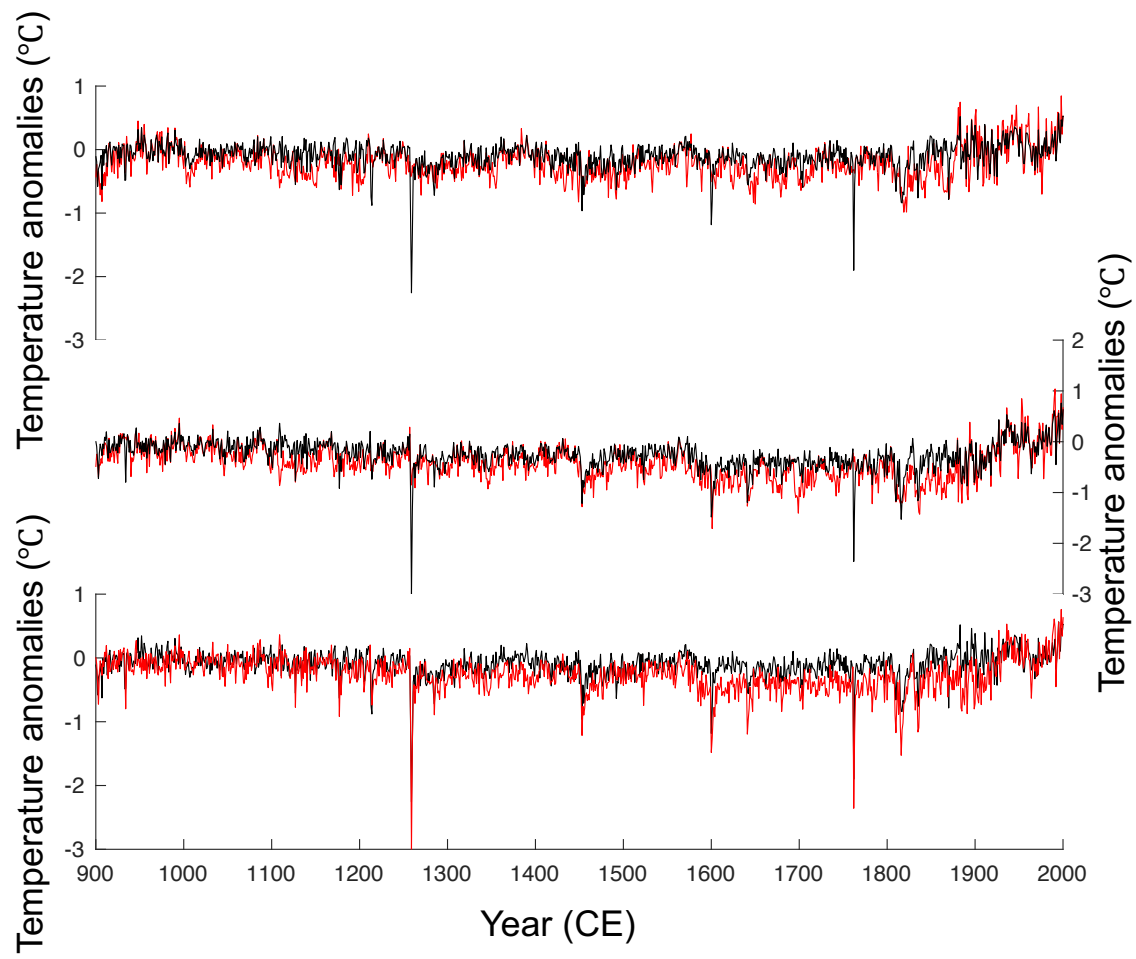
41 **Fig. S3.** Comparison of the composited summer temperature anomalies (unit: $^{\circ}\text{C}$, with respect to
42 1961–1990 CE) over the period 900–2019 CE in the (a) Qinghai–Tibetan Plateau and (b) Arctic.
43 The gray line is the uncertainty.



44

45 **Figure S4.** Comparison of the proxy reconstructed summer temperature anomalies (unit: $^{\circ}\text{C}$, with
 46 respect to 1961–1990 CE) over the period AD 900–2003 in the Arctic (red line) and in Europe
 47 from Luterbacher et al. (2016) (black line). (a) The raw data, (b) 100-year moving average, where
 48 the dashed lines are the 100-year (AD 1920–2019) average temperatures, and (c) 100-year moving
 49 correlation of the proxy reconstructed temperatures. The blue shaded bars indicate the transitions
 50 from weak to strong temperature correlations.

51



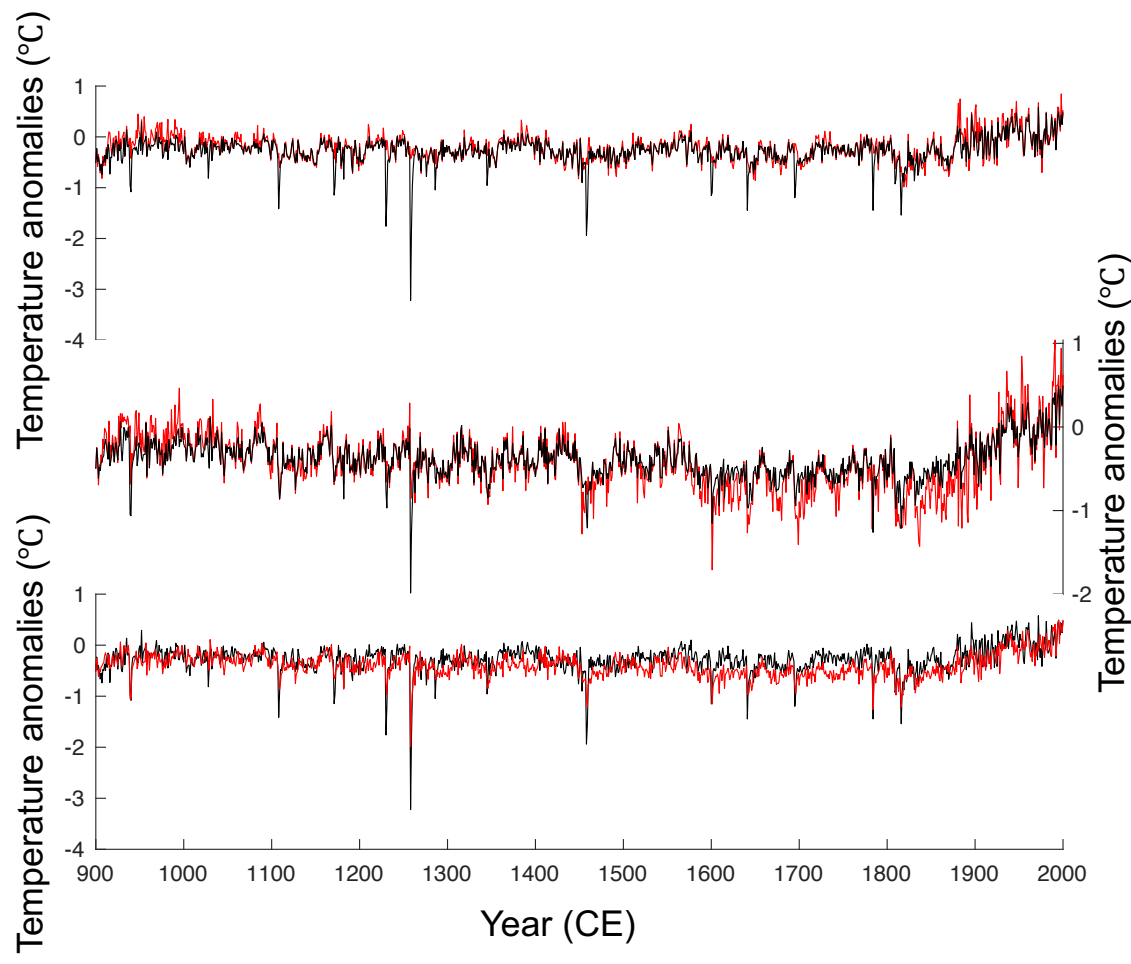
52

53 **Figure S5.** Comparison of the proxy reconstructed (red line) and data assimilation-based (black
 54 line) summer temperature anomalies (unit: $^{\circ}\text{C}$, with respect to 1961–1990 CE) using the CESM-
 55 LME simulation in the (a) Qinghai–Tibetan Plateau and (b) Arctic. (c) Comparison of the data
 56 assimilation-based temperature anomalies using the CESM-LME simulation in the Qinghai–
 57 Tibetan Plateau (black line) and Arctic (red line).

58

59

60



61 **Figure S6.** Same as Fig. S5, but using the LOVECLIM-LCE simulation for data assimilation.